Thermomechanical Fatigue FE Analysis Applied to High Temperature Metal Forming Processes

A. Escolán[a], J.M. Bielsa[a], M.A. Jiménez[a], R. Allende[b]

Instituto Tecnológico de Aragón (ITA) [a], Productos Tubulares (PTSAU) [b]

Email: aescolan@ita.es

Abstract: In high temperature metal forming processes strong mechanical and thermal gradients in the formed material and in the tooling coexist. Such gradients have a negative influence in the tool life cycle. That influence occurs due to mechanical and thermal cyclic loads undergone during the production process. This factor leads to the appearance of cracks on the tool surface because of thermomechanical fatigue phenomenon. The presented work is focused on a specific manufacturing process of seamless steel tubes which includes three basic steps: backward extrusion, perforation and Pilger rolling mill. This process transforms a blank or ingot into a final seamless steel tube with specific dimensions and characteristics depending on market requirements. The objective of this paper is to present thermomechanical fatigue FE analysis. These studies have been carried out in order to improve tool life and to know the effect of some key parameters of the main manufacturing process. For this end, it has been done several series of coupled thermomechanical FE simulations of the three analyzed conforming steps using ABAQUS/Explicit solver. Moreover, it has been incorporated a post-processing subroutine which enables to predict the number of cycles until crack appearance (tool life). This subroutine includes a cumulative thermomechanical fatigue damage method of analysis where the damage is treated as a combination of three factors: multiaxial fatigue, oxidation and creep. In the multiaxial fatigue, it has been studied, for each element which belongs to the surface, the critical level of crack initiation and propagation; in the oxidation and creep phenomena, it has been evaluated the ratio between mechanical and thermal cycles dependence (i.e. in phase or out of phase).

Keywords: Failure, Thermo-mechanical Fatigue, Forming, Fracture, ABAQUS/Explicit.

1. Introduction

The large dimension and high temperature tube forming is a process which includes several forming stages. The initial *ingot* is transformed by the mechanical and thermal action of the tooling in a *tube* with mechanical and geometrical characteristics depending on market requirements. In these steps co-exist strong mechanical and thermal gradients which enable the forming process.

All kind of forming process is conditioned by the presence of damage phenomena. On the one hand, sometimes the damage is a limiting factor of the process; on the other hand, its presence is necessary to enable the forming stage. In the manufacturing process, surface tooling directly interacts with the conformed material which is affected by such solicitations. This fact, together with the repeatability of the process, enhances the occurrence of surface cracks related to thermo-mechanical fatigue phenomena. Consequently the tool life is shortened.

This paper presents:

- A methodology for the fully coupled FE thermomechanical analysis of the three main stages of the tube forming process: Reverse extrusion, drilling and Pilger rolling. This methodology will provide knowledge in detail for both: the shaped material and the tooling.
- Fundamentals of cumulative thermomechanical fatigue damage models for fatigue life prediction.
- Thermomechanical fatigue life prediction by user subroutine scripting. This possibility of analysis has been added to the simulation methodology developed.

The presented FE simulation methodology includes the following features:

- Three-dimensional models solved with explicit integration in order to reach high computational efficiency, due to the size of the models and the complexity of the boundary conditions.
- Fully coupled thermo-mechanical analysis, including in it the tooling.
- Material model behavior including isotropic plasticity (hardening) and its temperature dependence.
- Heterogeneous damage model based on an initiation and evolution law.
- Adaptive meshing (ALE) and 'oriented mesh' in order to avoid significant distortion in elements quality.
- Deformable mesh for the tooling.
- Heat transfer by conduction in the contact-shaped material tooling and radiative heat transfer between the shaped material and the environment.
- Heat generation by plastic deformation of the shaped material and friction in the contact-shaped material tooling.

2. Metal forming process description

The hot tube process analyzed consists of a series of forming stages in order to obtain a tube with the dimensions and clearances required. Next, the three main stages analyzed are described.

2.1 Reverse extrusion

In the first stage, reverse extrusion (figure 1), the solid ingot at high temperatures is introduced in the matrix. After the performance of the vertical press, the plug enters over the upper part of the ingot and it penetrates until the base. In this process a preformed tube with a solid base is generated. The solid base breakage occurs in the second stage. The conformed material gets the cast shape which defines the exterior diameter of the generated shape. The internal diameter is defined by the diameter of the plug.

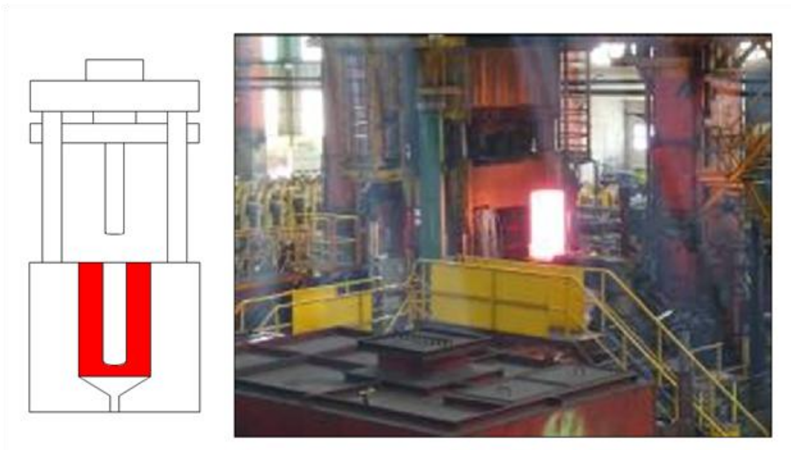

Figure 1. Reverse extrusion stage.

2.2 Perforation

In the second stage, perforation (figure 2), the blank resultant of the reverse extrusion, is pulled due to the action of the rolls. The rolls are turning on its axis and they are placed forming a conical configuration. The position of the rolls and the plug defines the exterior and interior tube diameter, respectively. Finally, the solid blank base is broken by the plug. The result is a tube preform which serves as an input in the third stage, Pilger rolling.

Figure 2. Perforation stage.

2.3 Pilger rolling

In the third stage, Pilger rolling (figure 3), the tube obtained from the perforation stage is rolled several steps. The thickness of the tube is reduced due to the action of the rolls which have a variable section. The action of the rolls defines the external diameter of the resultant tube; the internal diameter is defined by the diameter of the bar.

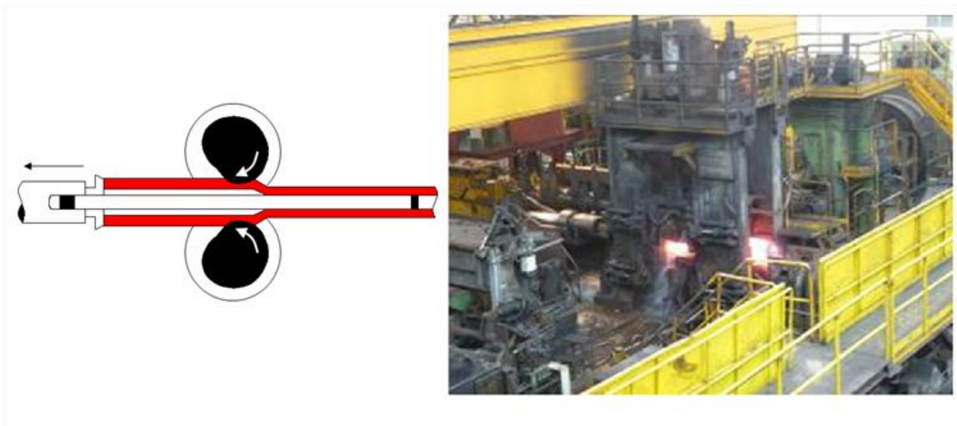

Figure 3. Pilger rolling stage.

3. Fundamentals of cumulative thermomechanical fatigue damage model

Thermomechanical fatigue has been analyzed by several authors by means of the implementation of damage rate models which include different physical effects. In example Neu/Sehitoglu's model includes three possible damage mechanisms: fatigue, environment (oxidation), and creep (Neu, 1989). This model differences between TMF IF (in-phase) and TMF OP (out of phase). When the maximum tensile load and peak cycle temperature occurs at the same time it is said that cycles are in phase (IP); by contrast, when the maximum tensile load and lowest cycle temperature coincide it is said that cycles are out of phase (OP). In TMF OP the oxidation damage mechanism becomes relevant, nevertheless creep damage mechanism is negligible; that is why voids growth is suppressed in compression. In TMP IP all three damage mechanisms are important (Minichmayr, 2008).

The total damage is expressed as:

$$D^{total} = D^{fatigue} + D^{oxidation} + D^{creep}$$

Equivalently, the total number of cycles can be formulated as:

$$\frac{1}{N^{total}} = \frac{1}{N^{fatigue}} + \frac{1}{N^{oxidation}} + \frac{1}{N^{creep}}$$

Damage due to oxidation reflects the repeated formation of an oxide layer at the crack tip and its rupture.

$$\frac{1}{N_f^{oxidation}} = \left[\frac{h_{cr}\delta_o}{B\Phi^{ox}K_p^{eff}}\right]^{-\frac{1}{\beta}} \frac{2(\Delta\varepsilon_{mech})^{(\frac{2}{\beta}+1)}}{\dot{\varepsilon}^{1-(\alpha/\beta)}}$$

where h_{cr} and δ_o are material parameters related to the critical oxide layer thickness and its ductility, respectively. α is a strain rate sensitivity parameter. β shows the exponential growth of the oxide layer. B is related with the generated crack length. K_p^{eff} is an effective oxidation constant related to the oxidation rate. This term takes into account the temperature history during the cycle time, t_c; it is defines as:

$$K_p^{eff} = \frac{1}{t_c}\int_0^{t_c} D_o exp\left(-\frac{Q_{ox}}{RT(T)}\right) dt$$

where D_o is the diffusion constant and Q_{ox} is the activation energy required. Also the relation between mechanical and thermal strains is included by means of the phasing factor ϕ^{ox}. The sensitivity of this factor is adjusted with the constant ξ^{ox}. This factor is equal to 0 for IP case and is equal to 1 for OP case.

$$\Phi^{ox} = \frac{1}{t_c}\int_0^{t_c} \phi^{ox} dt \quad \text{with} \quad \phi^{ox} = exp\left[-\frac{1}{2}\left(\frac{\frac{\dot{\varepsilon}_{th}}{\dot{\varepsilon}_{mech}}+1}{\xi^{ox}}\right)^2\right]$$

Damage due to creep is a diffusion process. It reflects the intergranular cracking and the growth of voids due to tension loading. To evaluate multiaxial states, damage is expressed as a function of effective stress $\bar{\sigma}$, hydrostatic stress σ_H, and drag stress K adjusting their sensitivity with the constants α_1 and α_2. The temperature dependence of the creep is included with an Arrenius function been A and ΔH experimental material constants, R the ideal gas constant and T the temperature.

$$\frac{1}{N_f^{creep}} = \Phi^{creep}\int_0^{t_c} A\ exp\left(-\frac{\Delta H}{RT(T)}\right)\left(\frac{\alpha_1\bar{\sigma} + \alpha_2\sigma_H}{K}\right)^m dt$$

Also the relation between mechanical and thermal strains is included by means of the phasing factor ϕ^{creep}. The sensitivity of this factor is adjusted with the constant ξ^{cr}.

$$\Phi^{creep} = \frac{1}{t_c}\int_0^{t_c} \phi^{creep} dt \quad \text{with} \quad \phi^{creep} = exp\left[-\frac{1}{2}\left(\frac{\frac{\dot{\varepsilon}_{th}}{\dot{\varepsilon}_{mech}}-1}{\xi^{creep}}\right)^2\right]$$

To evaluate multiaxial fatigue, it has been considered two multiaxial critical plane approaches.

The criterion proposed by Smith-Watson and Topper (SWT), (Smith, 1970) detects microcracks growth on planes of maximum tensile strain. His damage model is controlled by the strain range and maximum stress on the principal strain range plane.

$$\sigma_{n,max}\frac{\Delta\varepsilon}{2} = \frac{{\sigma_f}^2}{E}(2N_f)^{\ 2b} + \ {\sigma_f}'{\varepsilon_f}'(2N_f)^{\ b+c}$$

The criterion proposed by Fatemi-Socie (FS) includes the cyclic shear strain modified to include the crack closure effects.

$$\frac{\Delta\gamma}{2}\left(1 + k\frac{\sigma_{n,max}}{\sigma_y}\right) = \frac{\tau_f{}'}{G}(2N_f)^{\,b_y} + \ \gamma_f{}'(2N_f)^{\,c_y}$$

4. FE simulation models setup

To solve the problem, three-dimensional models solved with explicit integration (ABAQUS/Explicit) for high computational efficiency have been developed. This choice is due to the size of the models and the complexity of the boundary conditions.

The analysis has been defined as coupled thermo-mechanical, including in it the tooling and the blank. The material model has been considered as elasto-plastic including its dependence on temperature. Its behavior has been adjusted with the strain rate dependence based on experimental curves of the process.

In the second stage, perforation, it has been needed to include a damage model which complements the material definition in order to make possible the process of bottom breakage. The model combines ductile damage and shear damage. Breakage is governed by a damage initiation and evolution law. This phenomenon is illustrated in figure 4; in this figure a comparative between computational and real deformed shape is shown.

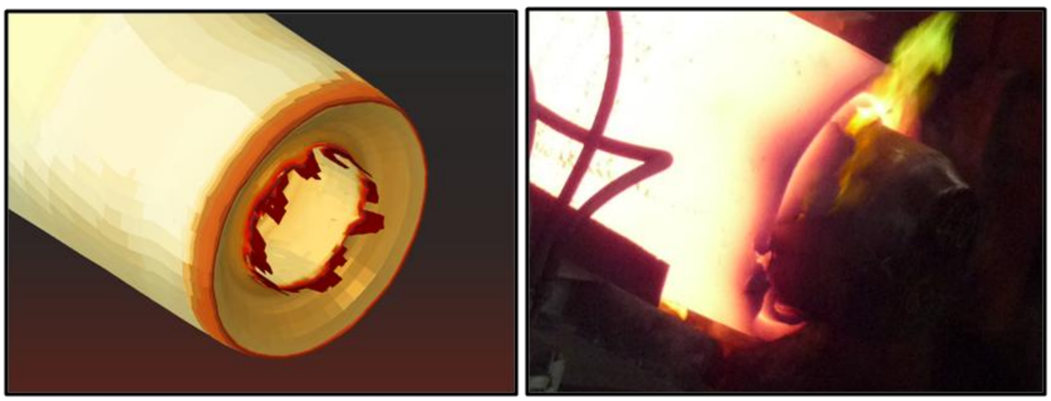

Figure 4. Damage model. Bottom breakage.

It has been employed C3D8RT elements in the models. On the other hand, the high levels of strain reached in the ingot led to the usage of three-dimensional ALE (Adaptive meshing technique) combined with initial 'oriented mesh' techniques. The aim is to avoid significant distortion keeping the quality of the elements. Figure 5, shows an example of the mesh evolution according to the plug penetration.

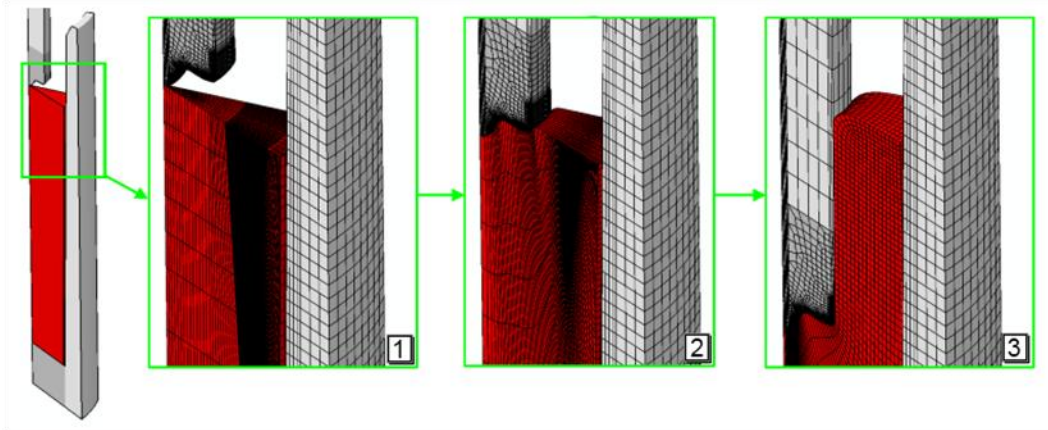

Figure 5. ALE technique in the reverse extrusion stage.

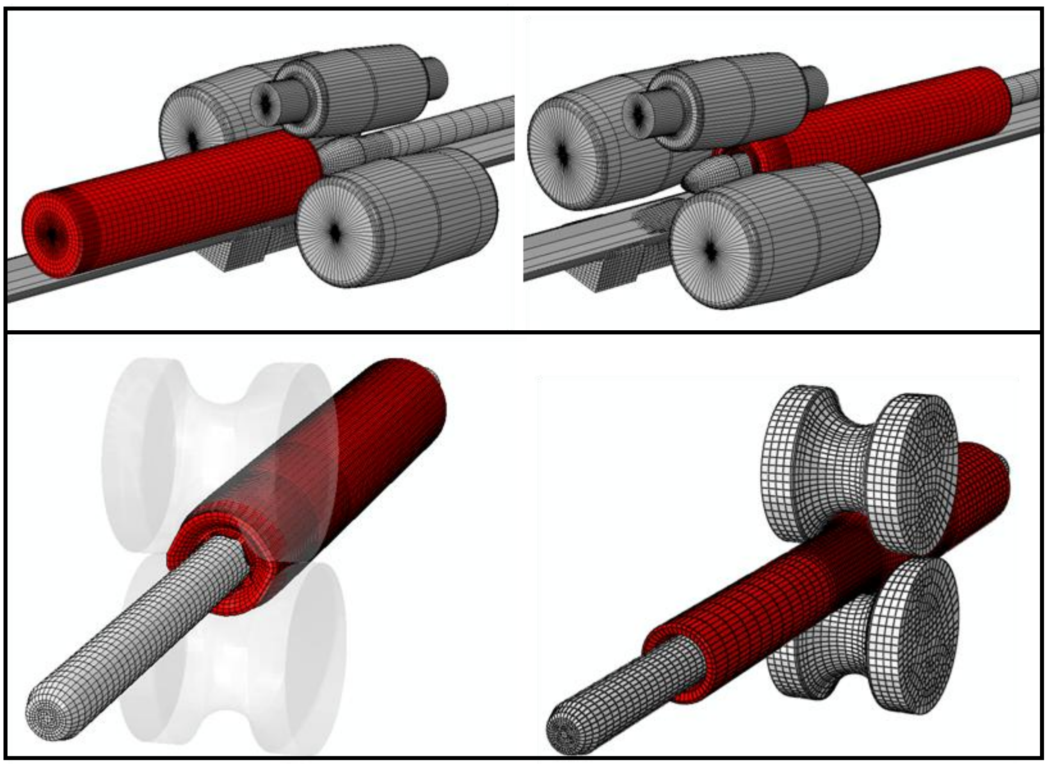

Figure 6. FEM models: 2nd stage - perforation (upper), 3rd stage Pilger - rolling (lower).

Finally, it has been defined thermomechanical interactions between tool and conformed material. Mechanical interactions have been defined by means of Coulomb's friction. Thermal interactions have been included defining heat transfer by conduction in the contact-shaped material tooling and radiative heat transfer between the shaped material and the environment. Moreover, heat generation by plastic deformation of the shaped material has been considered. Also, thermal expansion is considered.

Simulation models have been validated by comparing obtained deformed shapes, required forces, power curves (figure 7) and thermomechanical states between computational and experimental results.

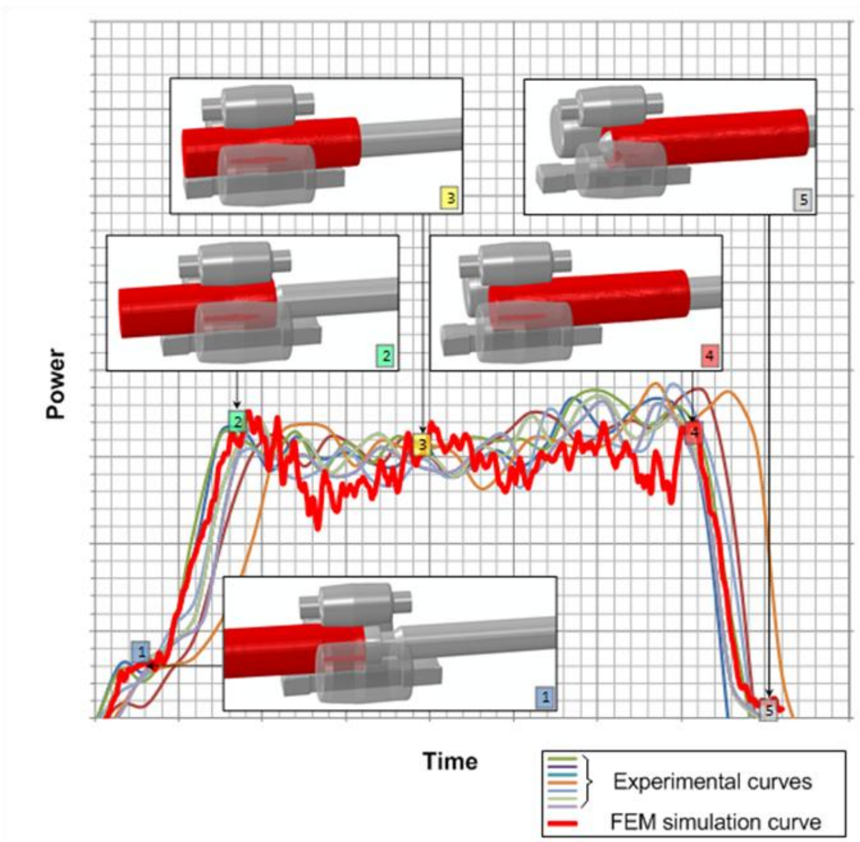

Figure 7. Required power in perforation stage. Experimental curves vs FEM simulation curve.

5. Thermomechanical fatigue analysis

The thermomechanical fatigue model presented in section 3 has been implemented in a user subroutine (vusdfld). The surface of the tool in each stage has been studied. This FORTRAN subroutine takes as an input the thermomechanical values obtained during the coupled thermomechanical analysis. In each calculation increment, multiaxial fatigue is evaluated by studying the most critical plane combinations considering the Fatemi Socie model (Fatemi, 1988) and the Smith-Watson and Topper model (Smith, 1970). It has been considered four different critical plane combinations as it is shown in figure 8. Moreover oxidation and creep damage is investigated according to expressions formulated in section 3.

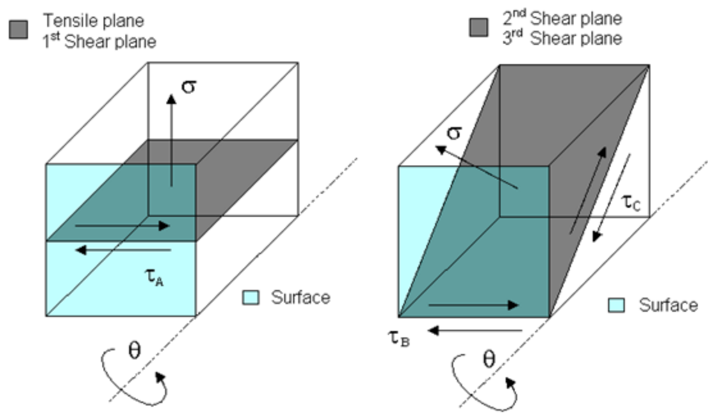

Figure 8. Critical planes.

According to section 3, the total number of cycles has been estimated as:

$$\frac{1}{N^{total}} = \frac{1}{N^{fatigue}} + \frac{1}{N^{oxidation}} + \frac{1}{N^{creep}}$$

For each element of the surface, the percentage of each physical effect considered has been evaluated.

All the TMF material parameters have been obtained from (Sehitoglu, 1990).

6. Computational results in terms of fatigue live critical areas

Next, obtained TMF prediction results are included in figures 9, 10 and 11 for the three analyzed forming stages. As it is shown, there is a good correlation between predicted damage zones and observed damage zones. These investigations have been carried out with industrial support and so data are qualitatively presented hereafter in order to meet the confidential requirements.

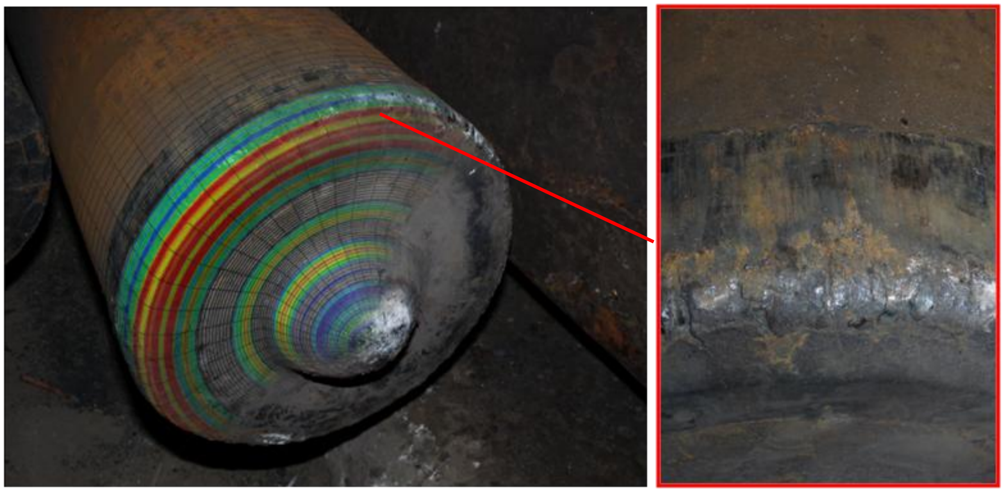

Figure 9. TMF prediction in the reverse extrusion plug.

The areas most affected by TMF phenomena are colored in red. These areas are estimated according to the number of cycles predicted by the programmed vusdfld subroutine.

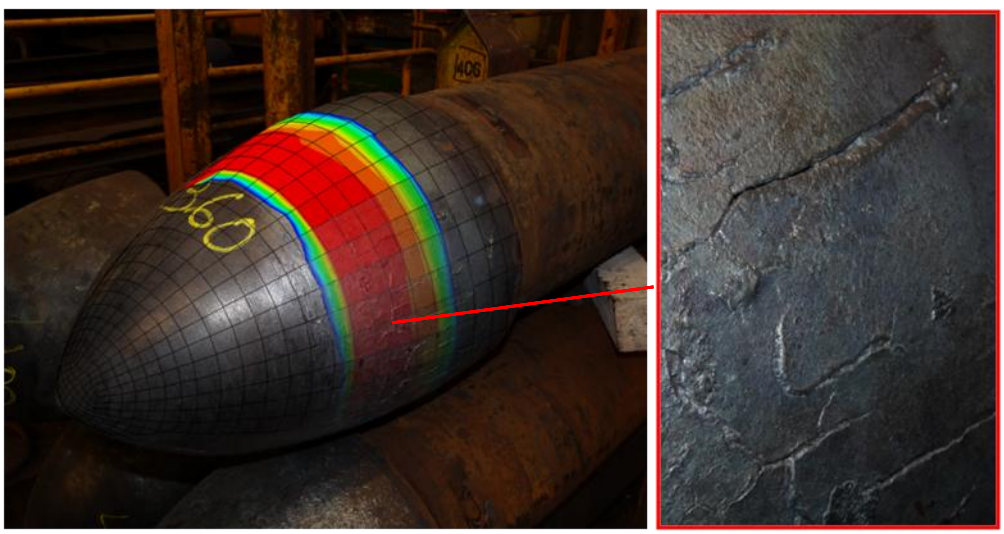

Figure 10. TMF prediction in the perforation plug.

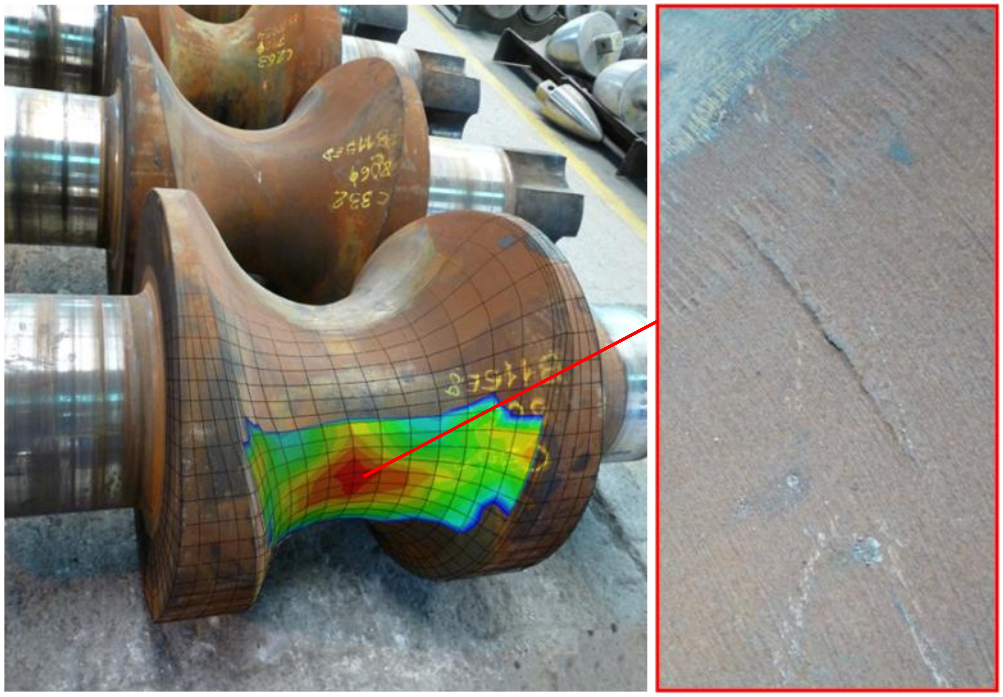

Figure 11. TMF prediction in the Pilger rolls.

For calculations it has been employed a 12 CPUs computer with a CPU frequency of 3.46 GHz. The needed time for calculations is included in table 1:

Stage	***Model***	***Parallelization***	***Time [hours]***
Reverse extrusion	Axisymmetric	4CPUs	2
Perforation	3D	4CPUs	140
Pilger rolling	3D	4CPUs	40

Table 12. Computation time.

7. Conclusions

The present paper proposes an approach for TMF analysis of tools involved in high temperature metal forming processes by means of FE simulations.

The developed methodology includes:

- Adaptive meshing technique (ALE) and fully coupled thermomechanical FE analysis.
- Thermomechanical fatigue life cycle prediction by means of a cumulative TMF damage model. Multiaxial fatigue, oxidation and creep have been considered. Predictions have been calculated by means of a vusdfld subroutine which interacts with the coupled thermomechanical analysis taking, as an input, thermo-mechanical values.

Obtained results are in good agreement with observed damaged zones for the three forming stages analyzed.

8. Acknowledgement

The authors would like to acknowledge the Spanish Center for the Development of Industrial Technology (CDTI) for the financial support and the company Productos Tubulares (PTSAU) for the permission to publish this work.

9. References

1. Abaqus Users Manual, Version 6.11-1, Dassault Systémes Simulia Corp., Providence, RI.
2. Fatemi A., and Socie, D.F., A Critical Plane Approach to Multiaxial Fatigue Damage Including Out-of-Phase Loading. Fatigue and Fracture of Engineering Materials and Structures. Vol.11. No. 3, 149-166, 1988.
3. Minichmayr R., Riedler M., Winter G., Leitner H., Eichlseder W. Thermo-mechanical Fatigue Life Assesment of Aluminium Components Using the Damage Rate Model of Sehitoglu. Internal Journal of Fatigue 30. 298-304, 2008.
4. New R.W., Sehitoglu H. Thermomechanical Fatigue, Oxidation, and Creep. Part I. Damage Mechanisms. Metallurgical Transations. A Physical Metallurgy and Materials Science. 20:1755-1767, 1989.
5. New R.W., Sehitoglu H. Thermomechanical Fatigue, Oxidation, and Creep. Part II. Damage Mechanisms. Metallurgical Transations. A Physical Metallurgy and Materials Science. 20:1769-1783, 1989.
6. Sehitoglu H., Boismier D.A., Thermo-mechanical fatigue of MAR-M247. Part 2. Life Prediction. Journal of Engineering Materials and Technology. Transactions of the ASME. 112:80-89, 1990.
7. Smith R.N., Watson P., and Topper T.H., A Stress-Strain Parameter for the Fatigue of Metals. Journal of Materials. Vol. 5. No. 4, 767-778, 1970.